Effective coordination as a predictor of adsorption energies: A model study of NO on Rh(100) and Rh/MgO(100) surfaces

Raghani Pushpa,[1] Prasenjit Ghosh,[2,3] Shobhana Narasimhan,[2] and Stefano de Gironcoli[1]
[1]*Scuola Internazionale Superiore di Studi Avanzati (SISSA) and CNR-INFM DEMOCRITOS, Via Beirut 2/4, I-34014 Trieste, Italy*
[2]*Jawaharlal Nehru Centre for Advanced Scientific Research, Jakkur P.O., Bangalore 560 064, India*
[3]*The Abdus Salam International Centre for Theoretical Physics (ICTP), Strada Costiera 11, I-34014 Trieste, Italy*
(Received 10 October 2008; revised manuscript received 2 February 2009; published 6 April 2009)

We have studied the adsorption of NO, and the coadsorption of N and O, on four physical and hypothetical systems: unstrained and strained Rh(100) surfaces and monolayers of Rh atoms on strained and unstrained MgO(100) surfaces. We find that as we go from Rh(100) to Rh/Mg0(100), via the other two hypothetical systems, the effective coordination progressively decreases, the *d* band narrows and its center shifts closer to the Fermi level, and the strength of adsorption and coadsorption increases. Both the strain and the presence of the oxide substrate contribute significantly to this. However, charge transfer is found to play a negligible role due to a canceling out between donation and back-donation processes. Our results suggest that lowering the effective coordination of Rh catalysts by strain, roughening, or the use of inert substrates might lower activation energies for the dissociation of NO.

DOI: 10.1103/PhysRevB.79.165406 PACS number(s): 28.52.Fa, 68.43.Bc, 96.12.Kz, 71.20.Be

I. INTRODUCTION

Though catalysts are crucial to the operation of many industrial and commercial processes, our understanding of the factors that make a good catalyst is still incomplete. Both the electronic and geometric structures of the catalyst are known to be important, and in recent years, it has become evident that coordination number can have a large effect on catalytic activity. The general understanding is that lower coordination leads to higher activity, though there are exceptions.[1] Industrial catalysts usually consist of small particles supported on a substrate. The presence of the substrate introduces additional factors, such as charge transfer between the catalyst and the support, change in the local environment of catalyst atoms, and geometrical strain imposed by the presence of the substrate. In this paper, we study some of these issues for a paradigmatic reaction, namely, NO dissociation on Rh, which is a crucial step in the reduction of nitrogen monoxide to nitrogen, for example, in three-way catalysts in automobiles. Rh is perhaps the best catalyst for this process,[2] but it is also by far the most expensive precious metal. It is therefore desirable to gain a better understanding of what makes Rh a good catalyst for this process so as to guide one in developing new catalysts that use less or no Rh.

Catalysts work by reducing activation barriers of chemical reactions. Though such barriers can nowadays be calculated by first-principles methods, the computations involved are expensive, and one would therefore like to correlate catalytic activity with some more easily accessible quantities. One such reactivity indicator that has been proposed is the binding energies of the products that, according to the Brønsted-Evans-Polanyi relationship, linearly correlate with the activation energy; it has been shown that this relationship holds for many systems.[3] Another useful quantity to examine is the position of the metal *d*-band center;[4] the closer this lies to the Fermi energy, the larger is the magnitude of the adsorption energy and, hence, surface reactivity. We show here that the "effective coordination" of Rh surface atoms can serve as a predictor for NO molecular adsorption strength in a variety of environments.

We consider the adsorption of NO, as well as the coadsorption of N and O, on a number of realistic and hypothetical Rh(100) surfaces. These configurations constitute the initial and final states in the dissociation of NO. In an attempt to gauge the contributions made by the chemical nature of the substrate, as well as strain, we have studied adsorption and coadsorption on four kinds of (100) surfaces: (i) the surface of an unstrained Rh crystal; (ii) the surface of a Rh crystal that has been stretched (expanded) so as to be commensurate with an MgO(100) surface; (iii) a monolayer of Rh on Mg0(100), with both the Rh and the substrate's in-plane spacing fixed to be that of Rh(100); and (iv) a monolayer of Rh on MgO(100), with all in-plane spacings fixed to be that of MgO(100). Note that straining systems (i) and (iii) leads to systems (ii) and (iv), respectively, while changing the substrate from Rh to MgO converts systems (i) and (ii) to systems (iii) and (iv), respectively.

We emphasize that the purpose of our study is to alter the Rh environment in a simple and systematic way in order to extract trends; we do not necessarily claim that these systems are physically realizable. Indeed, while system (i) is certainly realizable, both systems (ii) and (iii) are clearly hypothetical. As for system (iv), it is not yet known experimentally whether or not the Rh layer wets the oxide pseudomorphically. However we expect that the conclusions drawn from the study of these systems should apply also to the real catalyst.

The reactivity of surface Rh atoms is presumably sensitive to three factors: (a) the number of neighbors, (b) the chemical nature of these neighbors, and (c) the distance at which these neighbors are situated. One quantity that encapsulates all three of these is the "effective coordination number," which we define as

$$n_e(i) = \Sigma_j \rho_j^{\mathrm{at}}(R_{ij}) / \rho_{\mathrm{Rh}}^{\mathrm{at}}(R_{\mathrm{bulk}}), \tag{1}$$

where $\rho_j^{\mathrm{at}}(R)$ is the atomic charge density of an isolated atom j (Rh, O, or Mg in our case) as a function of R, the distance

from its nucleus, and the sum is taken over all the nearest-neighbor atoms j around a surface Rh atom i. R_{ij} is the distance between atoms i and j, and R_{bulk} is the nearest-neighbor (NN) distance for bulk Rh. With this definition the effective coordination becomes equal to the nominal coordination of 12 for a Rh atom in the bulk. The effective coordination is a measure of the ambient electron density for each atom, which plays a crucial role in determining local energetics in semiempirical approaches such as the embedded-atom method,[5,6] the effective medium theory,[7] or the glue model.[8] Recently it has been shown that this parameter can be used to rationalize trends in surface core level shifts when undercoordinated Rh atoms assume a variety of geometries.[9] In the present case, the effective coordination of surface atoms is progressively lowered as one proceeds from system (i) to system (iv), as we will show further below.

Another factor—magnetism—seems likely to play a role in these systems. Bulk Rh is "almost" ferromagnetic. There has been a long-running controversy over whether or not the Rh(100) surface is magnetic;[10–14] however it seems clear that Rh monolayers and clusters are magnetic.[15–18] This raises the question of what possible role magnetism may play in the operation of Rh catalysts; this issue is also dealt with in this paper. Though the adsorption of NO on Rh(100) has been studied by previous authors,[1,2,19] we are not aware of any systematic program of calculations that is similar in spirit to ours.

II. METHOD

Our calculations have been performed using *ab initio* density-functional theory, using the PWSCF package of the Quantum-ESPRESSO distribution.[20] The spin-polarized (SP) version of the Kohn-Sham equations was solved using ultrasoft pseudopotentials[21] and a plane-wave basis with a cutoff of 30 Ry. Exchange and correlation effects were treated using the generalized gradient approximation in the form suggested by Perdew, Burke, and Ernzerhof.[22] In order to improve convergence, a Methfessel-Paxton smearing[23] with a width of 0.03 Ry was used.

Most results for the Rh(100) and Rh/MgO(100) slabs were obtained by using a (1×1) asymmetric supercell. For cases (i) and (ii) this contained four Rh layers of which the outermost two (toward the adsorbate) were allowed to relax, while the inner two were kept fixed at the appropriate bulk separation. However, some tests were also performed with symmetric slabs containing eight layers of Rh atoms. Brillouin-zone integrations for such (1×1) surface cells were carried out using a $(12\times12\times1)$ Monkhorst-Pack mesh.[24]

The adsorption and coadsorption studies were carried out using slabs with larger unit cells, [viz., (2×2) and (2×3)], together with corresponding k-point meshes [$(6\times6\times1)$ and $(6\times4\times1)$, respectively]. For systems (i) and (ii), we found that a slab containing four Rh layers was sufficient to give well-converged adsorption energies; however, for one particular adsorption geometry, we found it necessary to use a slab with five Rh layers. All the results presented below for adsorption and coadsorption on systems (iii) and (iv) were obtained using a slab containing one layer of Rh atoms over four MgO layers.

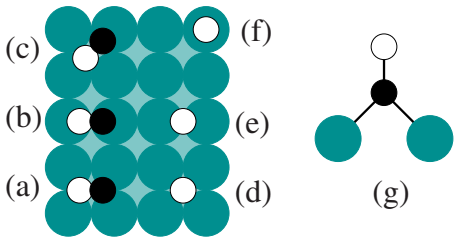

FIG. 1. (Color online) Schematic diagrams showing the geometries considered for adsorption studies. The cyan (gray), white, and black circles represent Rh, O, and N atoms, respectively. The NO occupies different sites and is oriented differently in the six cases depicted here. (a), (b), and (c) show top views of configurations where the NO sits horizontally on the Rh substrate, while (d), (e), and (f) show top views of configurations where the NO sits vertically on the substrate; in these, the N atoms are not visible as they sit directly below the O atoms. The picture (g) shows a side view of configuration (e).

In adsorption studies, six different geometries were considered; these are shown in Fig. 1, while Fig. 2 shows the three different geometries for the coadsorption studies. These two figures show (schematically) the geometry prior to relaxation; after relaxation (in the absence of symmetry constraints) the geometries remained roughly similar, though bond lengths changed.

As we will show in Sec. III, in cases (ii), (iii), and (iv), the Rh(100) surface was found to be magnetic. For case (ii), one needs to worry about the possibility that the bottom surface acquires a magnetic moment and is thus no longer representative of a bulklike layer. To mitigate this, in these cases we deposited a layer of H atoms on the bottom surface, which has the effect of quenching magnetization on that surface.

III. RESULTS

A. Preliminary tests: bulk Rh, bulk MgO, and gas-phase NO

We obtained a value of 3.85 Å for the lattice constant of bulk Rh, which is in excellent agreement with the experimental value of 3.80 Å (Ref. 25) and previous theoretical values of 3.87 Å.[26] Our value implies that the distance be-

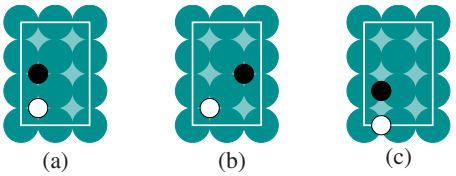

FIG. 2. (Color online) Top view of the geometries considered for N and O adsorption on Rh(100) surfaces. The cyan (gray), white, and black circles represent Rh, O, and N atoms, respectively. In configuration (a), N and O are at nearest-neighbor hollow sites; in (b) N and O are at diagonally opposite hollow sites. In configuration (c), N and O are at the bridge sites between two Rh atoms. The white rectangle indicates the 2×3 unit cell used for coadsorption studies.

tween NN Rh atoms on the (100) surface is 2.73 Å, while the interlayer distance between bulklike layers in a Rh(100) slab is 1.93 Å.

For MgO, we obtained a lattice constant of 4.25 Å, which is identical to the value obtained in previous calculations[27] and is in good agreement with the experimental value of 4.21 Å.[28] Note that this would imply that if a Rh monolayer were to be deposited commensurately with an MgO(100) substrate, the NN Rh-Rh distance within the monolayer would be increased to 3.00 Å, which corresponds to a strain of 9.9%.

For NO in the gas phase, we obtained a binding energy of 7.13 eV and an N–O bond length of 1.17 Å. For comparison, the experimental values are 6.5 eV and 1.15 Å, respectively.[29] In all these cases, it can be seen that our results are in good agreement with both experiments and previous calculations, lending support to the validity of our approach.

B. Case (i)—unstrained Rh(100) surface

For the surface energy of the clean and unstrained Rh(100) surface [case (i)], we obtain a value of 1.12 eV/surface atom, which agrees exactly with the value obtained in a previous calculation[26] and is also in reasonably good agreement with the experimental value of 1.27 eV/surface atom.[30] We find that the first interlayer spacing d_{12} is contracted by 3.5% with respect to the bulk interlayer spacing of 1.93 Å; this is similar to the contraction of 4.0% found in an earlier study[26] but more than the contraction of $1.4\% \pm 1.4\%$ reported experimentally.[30] We find that the next two interlayer spacings, d_{23} and d_{34}, are both expanded by 0.77%; the next interlayer spacing d_{45} is very close to the bulk interlayer spacing. We find that the surface is not ferromagnetic, which is in agreement with several previous studies,[13,14] though it disagrees with some reports in the literature.[10,11]

For case (i), we find that the effective coordination $n_e = 8.49$. This is slightly increased with respect to the nominal surface coordination (the number of nearest-neighbor atoms for a surface atom) of 8, due primarily to the contraction of d_{12} relative to the bulk interlayer spacing.

We define the adsorption energy as $E_{\mathrm{ads}} = E_{\mathrm{NO:Rh(100)}} - E_{\mathrm{Rh(100)}} - E_{\mathrm{NO}}^{\mathrm{gas}}$, where E is the value obtained from *ab initio* calculations for the total energy of the corresponding configuration. In agreement with previous results,[2,26] we find that the most favorable adsorption geometry on an unstrained Rh(100) slab is the "vertical bridge" (VB) [corresponding to Figs. 1(e) and 1(g); the adsorption geometry is also shown in Fig. 3(a)]. With a (2×2) unit cell (i.e., a coverage of 1/4 ML), we obtain $E_{\mathrm{ads}} = -2.59$ eV in this geometry; the N–O bond length is increased slightly from the gas-phase value of 1.17 to 1.20 Å. The next most favorable adsorption geometry is the "horizontal hollow" (HH) [see Fig. 1(a)] with $E_{\mathrm{ads}} = -2.47$ eV and an N–O bond length of 1.31 Å. The details of the adsorption geometries for both VB and HH are given in Table I. All these values are in excellent agreement with a previous study.[26]

We have also investigated the geometry and energetics of the coadsorption of N and O on this surface. We find that both N and O prefer to occupy fourfold hollow sites, as has also been reported in a previous paper.[19] In Table II, we show how the coadsorption energy, defined as $E_{\mathrm{coads}} = E_{\mathrm{N+O:Rh(100)}} - E_{\mathrm{Rh(100)}} - E_{\mathrm{NO}}^{\mathrm{gas}}$, varies with adsorbate coverage and adsorption geometry. We find that the N and O atoms prefer to occupy next-nearest-neighbor (NNN) hollow sites over nearest-neighbor hollow sites. Also, the magnitude of E_{coads} increases as the coverage is decreased. These observations suggest that there is a repulsive interaction between the N and O atoms after dissociation of NO. We note that in a previous study,[19] a coadsorption energy of −3.50 eV was obtained at a coverage of 1/16 ML, which is in keeping with our conclusions here.

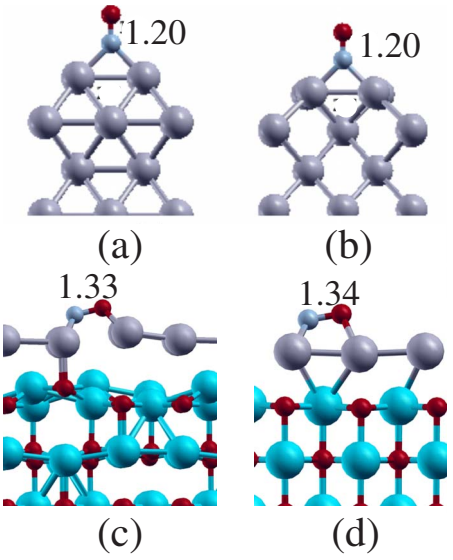

FIG. 3. (Color online). The most stable configurations for adsorbed NO in (a) case (i), (b) case (ii), (c) case (iii), and (d) case (iv). In cases (i) and (ii), vertical configuration of NO at a bridge site is the most stable; whereas in cases (iii) and (iv), horizontal configuration at the hollow site is the most stable. Small blue (gray) and red (black), and large gray and turquoise spheres represent N, O, Rh, and Mg atoms, respectively. In (a) and (b), and in the first row of atoms in (c) and (d) the large gray spheres represent the Rh atoms. In (c) and (d) turquoise (gray) spheres in the second, third and fourth layers represent Mg atoms.

C. Case (ii)—stretched Rh(100) surface

When an in-plane expansion of 9.9% is imposed on a (1×1) Rh(100) slab, we find that the bulk interlayer spacing ($\approx d_{45}$) is reduced by 11.3% with respect to the unstrained case and becomes equal to 1.71 Å. Upon allowing all interlayer distances to relax in an eight-layer slab, the first three interlayer spacings d_{12}, d_{23}, and d_{34} are changed to 1.59, 1.76, and 1.73 Å, respectively. These are contracted significantly, with respect to the bulk interlayer distance in unstrained Rh(100), by 17.3, 8.9, and 10.5%, respectively. The net effect of having longer intralayer distances but shorter interlayer distances at the surface is that now the effective coordination $n_e = 6.65$, i.e., as a result of stretching, the effective coordination has decreased on going from case (i) to case (ii).

TABLE I. The Rh–Rh bond length ($d_{\text{Rh-Rh}}$), the Rh–N bond length ($d_{\text{Rh-N}}$), the Rh–O bond length ($d_{\text{Rh-O}}$) and the N–O bond length ($d_{\text{N-O}}$) of NO on different adsorption sites for the four cases. The number given below each case denotes the Rh-Rh in-plane distance for the clean surfaces. Rh_N and Rh_O indicate the distances between two Rh atoms bonded to N and O atoms, respectively. All distances are given in angstrom.

System	Site and geometry	$d_{\text{Rh-Rh}}$	$d_{\text{Rh-N}}$	$d_{\text{Rh-O}}$	$d_{\text{N-O}}$
Case (i)	VB	2.74	1.96		1.20
(2.73)	HH	2.75(Rh_N)	1.98	2.21	1.31
		2.79(Rh_O)			
Case (ii)	VB	2.70	1.96		1.20
(3.00)	HH	3.13(Rh_N)	1.98	2.22	1.32
		3.21(Rh_O)			
Case (iii)	VB	2.75	1.93		1.20
(2.73)	HH	2.70(Rh_N)	1.95	2.15	1.33
		2.95(Rh_O)			
Case (iv)	VB	2.56	1.94		1.21
(3.00)	HH	2.66(Rh_N)	1.95	2.18	1.34
		2.59(Rh_O)			

In Fig. 4, we show the layer-resolved magnetization per atom of a symmetric (1×1) stretched eight-layer slab (stars). Interestingly, the stretched Rh(100) surface is now magnetic with surface magnetization of 1.0 μ_B/atom. In order to reduce computational load, it is a common practice to consider asymmetric slabs where some of the bottom layers are fixed at their bulk positions. The circles in Fig. 4 show the magnetization per atom in a (1×1) four-layer slab with the bottom two layers fixed at 1.71 Å interlayer spacing and the top two layers relaxed. We find that only in the top two layers is the magnetization close to the one in the layers of the symmetric slab, and a "spurious" magnetization as large as 1.2 μ_B/atom is present on the frozen-geometry bottom surface. In order to quench this spurious magnetization, we considered also an asymmetric four-layer Rh slab where H atoms were adsorbed on the bottom surface. The results are again reported in Fig. 4 as squares, and we now find that the magnetic moments on all layers are very similar for the four-layer and eight-layer slabs, giving us confidence that adsorption energies obtained with the former will be accurate. The interlayer distances are also very similar in the eight-layer symmetric slab and in the four-layer slab with H adsorbed on the bottom surface but are (slightly but perceptibly) different on the four-layer slab without H on the bottom surface.

TABLE II. Dependence of coadsorption energy E_{coads} on coverage and adsorption geometry. The first row corresponds to a coadsorption of N and O in a 2×2 unit cell in next-nearest-neighbor hollow sites, while the second and third rows (a) correspond to results for the geometries depicted in Figs. 2(a) and 2(b), respectively. Here, C=coverage of N=coverage of O.

Coverage C	E_{coads} (eV)	$r_{\text{N-Rh}}$ (Å)	$r_{\text{O-Rh}}$ (Å)
1/4 ML	−3.20	2.03	2.14
1/6 ML (a)	−3.10	1.99, 2.10	2.04, 2.35
1/6 ML (b)	−3.34	2.03, 2.04	2.14, 2.17

Adsorbing H on the bottom surface also turns out to be crucial in correctly predicting the stable adsorption geometry for NO. In the absence of H, it is found that the VB and HH configurations are degenerate, with both having an adsorption energy of $E_{\text{ads}}=-2.83$ eV; however, when H is adsorbed on the bottom surface, the VB (with $E_{\text{ads}}=-2.86$ eV) is found to be clearly favored over the HH (with $E_{\text{ads}}=-2.71$ eV); for the reasons stated above, we believe that the set of numbers obtained with H atoms on the bottom surface is more to be trusted. This stable adsorption geometry is depicted in Fig. 3(b).

In order to gauge the effects of magnetism on adsorption energies, we also performed non-spin-polarized (NSP) calculations. We found that the magnitude of E_{ads} increases in the absence of magnetization; however, the difference between the VB and HH geometries is maintained: with NSP calculations, the former gives $E_{\text{ads}}=-2.96$ eV while the latter gives $E_{\text{ads}}=-2.82$ eV.

We found that NO adsorption leads to a significant distortion in the position of Rh atoms (see Table I). When NO is adsorbed in the VB configuration, the Rh-Rh distance for the

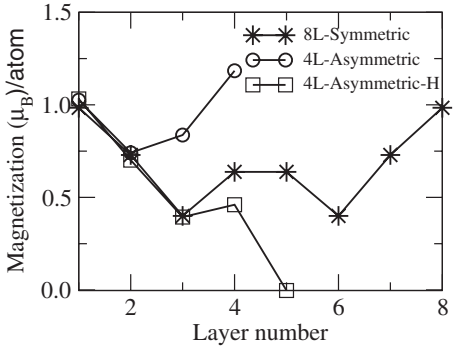

FIG. 4. Magnetization of the stretched Rh(100) surface [case (ii)] for an eight-layer symmetric slab (stars), a four-layer asymmetric slab (circles), and a four-layer asymmetric slab with H adsorbed at the bottom of the slab (squares).

two Rh atoms bonded to N is reduced significantly, from 3.00 to 2.70 Å. However, for the HH configuration, the distances between the two Rh atoms bound to N and O increase to 3.13 and 3.21 Å, respectively. The internal bond length in NO is increased in all cases: to 1.20 Å for the VB and to 1.32 Å for the HH configuration. Note that this also suggests that it might be easier to break the N–O bond in the HH configuration.

Next, we coadsorb N and O on this surface. The coadsorption geometries considered by us are shown in Fig. 2. When we start from a configuration where N and O are at NN hollow sites [see Fig. 2(a)], the O atom moves away from N and sits at the bridge site which is equidistant from the N atom and its image. This configuration represents the most favorable coadsorption geometry, with $E_{\mathrm{coads}}=-3.47$ eV. The second most favorable configuration is one where both N and O sit at NNN hollow sites [Fig. 2(b)]; here $E_{\mathrm{coads}}=-3.33$ eV. Unlike in case (i), the stretched Rh(100) surface also has a local minimum when both the atoms sit at bridge sites [see Fig. 2(c)]. This is the configuration that the system assumes just after the dissociation of NO and corresponds to $E_{\mathrm{ads}}=-3.24$ eV. As in case (i), the magnitude of E_{ads} is increased by ~0.3 eV in the first two adsorption geometries upon performing an NSP calculation; however, in the third case, E_{ads} is essentially unchanged. It is also worth noting that changes in interatomic distances are slight when comparing SP and NSP calculations.

D. Case (iii)—monolayer of Rh on MgO(100) at Rh(100) lattice constant

The third case we consider is again an artificial one. We consider first an MgO(100) substrate that has been strained (compressed) in plane so that it has the same in-plane lattice constant as in case (i). As a result of this in-plane compression, we find that the first two interlayer spacings are both increased by 8.15% relative to the interlayer spacing in unstrained MgO. There is also a noticeable rumpling of Mg-O layers near the surface. We define the rumpling as $\Delta z=(z_{\mathrm{O}}-z_{\mathrm{Mg}})/d_0$, where z_{O} and z_{Mg} are the z coordinates (normal to the surface plane) of O and Mg, respectively, and d_0 is the bulk interlayer spacing. The outermost MgO layer has $\Delta z=2.0\%$, while the second MgO layer has $\Delta z=-0.1\%$. Note that the rumpling is opposite in the two outermost layers: in the topmost layer, oxygen atoms are displaced further away from the substrate than Mg atoms, whereas for the second layer, the reverse is true.

When a monolayer of Rh is deposited pseudomorphically on this compressed MgO substrate, it binds with a binding energy E_{bin} of −3.59 eV/Rh atom. Here, the binding energy has been defined by $E_{\mathrm{bin}}=E_{\mathrm{Rh:MgO}}-E_{\mathrm{MgO}}-E_{\mathrm{Rh}}^{\mathrm{gas}}$, where $E_{\mathrm{Rh:MgO}}$ is the total energy of the Rh/MgO slab, E_{MgO} is the energy of the MgO slab alone, and $E_{\mathrm{Rh}}^{\mathrm{gas}}$ is the energy of an isolated Rh atom in the gas phase. The Rh atoms sit atop the oxygen atoms of the outermost MgO layer, with a Rh-O separation of 2.22 Å. The deposition of the monolayer changes both the rumpling and the relaxation of the outermost MgO layers. The first two layers now display a rumpling of −4.2% and 0.7%, respectively; note that the deposition of Rh has actually reversed the direction of rumpling. There is also a change in interlayer spacings, with the distance between the two outermost MgO layers now expanded by 9.55% relative to the interlayer distance in unstrained MgO, while the expansion of the next interlayer spacing is now reduced slightly, from the value of 8.15% (in the absence of the Rh adlayer) to 8.05%. The Rh monolayer in this case is found to be magnetic, with a magnetic moment of 1.5 μ_B/atom.

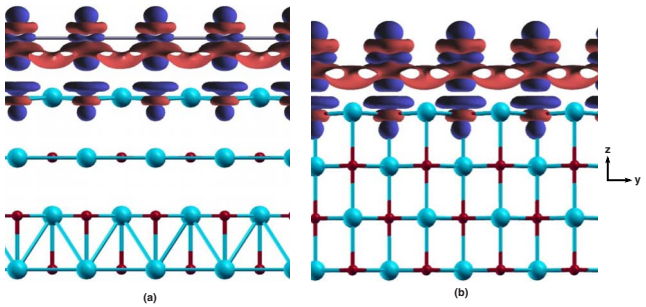

FIG. 5. (Color online) Charge redistribution on placing a monolayer of Rh atoms on an MgO substrate for (a) case (iii) and (b) case (iv). Red (light) and blue (dark) lobes represent regions where the electronic charge has increased and decreased, respectively. Red (black) and turquoise (gray) spheres represent O and Mg atoms, respectively; the gray Rh atoms are not visible because they are surrounded by charge-transfer lobes. Note that both the Rh overlayer and the O atoms in the topmost Mg-O layer display both red and blue lobes.

In principle, placing metal atoms on an oxide substrate can lead to charge transfer. In Fig. 5(a), we have plotted the redistribution of charge upon placing a layer of Rh atoms on an MgO substrate. In this figure, red (light) and blue (dark) regions represent areas where the electronic charge has increased and decreased, respectively. It is interesting to note that one observes *both* red (light) and blue (dark) lobes on both the Rh layer and the topmost Mg-O layer. This is because of the simultaneous presence of donation and back donation between the adsorbate (Rh) and the substrate (MgO), as is well known for such systems. Interestingly, these two processes essentially cancel out for this system; the net charge transfer, as calculated by Lowdin population analysis, is only 0.015 electrons per Rh atom between the Rh overlayer and the MgO substrate. The other interesting thing to note is the fact that there are lobes of electronic charge in the interstices between the Rh atoms and above top layer Mg atoms. This contributes to the electrostatic binding of the adlayer to the substrate. A similar binding mechanism has been suggested in the literature for metal adlayers on alumina substrates.[31]

The effective coordination n_e is now lowered to 5.51. Note that n_e is lower for both cases (ii) and (iii) relative to case (i); however, the lowering in case (iii) (which is due to the replacement of the Rh substrate by an MgO support) is more significant than in case (ii) (where it is due to stretching the system to the lattice constant of MgO). Similarly, the magnetic moment is larger in case (iii) than in case (ii).

Upon adsorbing NO on this compressed Rh/MgO(100) system, we find that the most favorable adsorption geometry

is the HH [depicted in Fig. 3(c)], with $E_{ads}=-3.38$ eV, which is larger in magnitude than the adsorption energy of −3.17 eV for the VB configuration. Note that this is in contrast to the most favored adsorption geometry for both cases (i) and (ii); it is now favorable for both N and O to bind to Rh atoms.

For the VB case, the distance between the two Rh atoms bound to the N (Rh_N) increases slightly from 2.73 to 2.75 Å. On the contrary, for the HH geometry, the distance between the same pair of Rh atoms decreases to 2.70 Å, while that between the Rh atoms attached to the O atom (Rh_O) increases to 2.95 Å. This is because, as a result of strong binding between NO and the Rh atoms, the Rh_N pair is pulled out of the surface.

Moreover, upon adsorbing NO, the magnetization of the Rh atoms is quenched. For the HH NO adsorption geometry, this reduction is as follows: for the two Rh atoms to which N is attached, the reduction is by 74%; for the two Rh atoms to which O is attached, it is by 45%; and for the two Rh atoms which are furthest from NO, the reduction is only by 9%. Once again, we find significantly enhanced binding upon performing an NSP calculation, with $E_{ads}=-4.07$ eV and −3.82 eV for the HH and VB geometries, respectively. The coadsorption energies are −4.64 and −3.32 eV when the N and O atoms are in the NN hollow [Fig. 2(a)] and bridge [Fig. 2(c)] sites, respectively.

E. Case (iv)—monolayer of Rh on MgO(100) at MgO lattice constant

Next we put a pseudomorphic layer of Rh atoms on an unstrained MgO(100) substrate. In reality it is possible that the Rh layer will reconstruct so as to reduce surface stress. We are not aware of any experimental data on this issue. However, as we have mentioned above, it is still useful to consider this hypothetical structure so as to establish trends. Assuming pseudomorphic wetting, we find that Rh atoms again preferentially occupy the sites atop O atoms. The binding energy for this configuration, defined as in case (iii), is found to be $E_{bin}=-3.27$ eV/Rh atom; this is somewhat less in magnitude than the value of −3.99 eV obtained in a previous study.[27] The Rh-O distance is found to be 2.25 Å, which is larger than the value of 2.10 Å reported earlier.[27] Both the Mg and O atoms in the topmost layer move outwards, away from the substrate, so that the mean interlayer distance between the top two MgO layers is increased by 0.73% relative to the bulk interlayer spacing. However, there is a considerable rumpling (Mg atoms are higher up on the surface than oxygen atoms, with $\Delta z=-4.0\%$) of the topmost MgO layer; this is in good agreement with one earlier reported value of −4.3% (Ref. 17) but somewhat less than the value of −6.1% obtained in another study.[27] The rumpling is reduced to +1.0% in the MgO layer below this one. Note that for both layers the rumpling is reversed with respect to that observed for a bare MgO(100) surface.

For a Rh atom in case (iv), we obtain $n_e=3.59$. Note that this is significantly lowered with respect to the value of 8.49 obtained in case (i) due to a combination of two factors: the replacement of substrate Rh atoms by Mg and O atoms and the stretching to the MgO lattice constant. If the topmost Rh layer were to relieve stress by forming a network of misfit dislocations, the value of n_e would be larger than this but presumably still quite low. If the Rh atoms were to clump up instead of wetting the surface, then the n_e of atoms at island edges would also be very low.

Once again, we find that the surface Rh atoms are magnetic, with a moment of 1.5 μ_B/atom. This is in marked contrast with the result reported in Ref. 32 where no magnetization was found for this geometry.

In Fig. 5(b), we present a plot of charge redistribution for the Rh/MgO system. From this figure, it is evident that, as in case (iii), there is both donation and back donation between the overlayer Rh atoms and the O atoms in the MgO substrate. Once again, these two processes effectively cancel out, and there is a net charge transfer of only 0.018 electron per Rh atom from the oxygen to the Rh atom. Again there is a significant lateral redistribution of electronic charge, quite similar to case (iii).

Next, we study the adsorption of NO on this Rh/MgO(100) system. As in case (iii) above, we find that it is now most favorable for the NO atom to lie horizontally on the surface: $E_{ads}=-4.08$ and −3.87 eV for the HH and VB geometries, respectively. In Fig. 3(d) we have depicted the lowest-energy adsorption geometry, corresponding to the HH configuration.

With the adsorption of NO on 1 ML of Rh on MgO, the Rh atoms to which the NO is attached come closer together for both the HH and VB geometries (see Table I). We speculate that this may be because Rh–Rh bonds are under considerable tensile stress when deposited pseudomorphically on MgO; the adsorption of NO breaks the symmetry and allows the Rh atoms bonded to NO to come closer together.

As in case (iii), upon adsorbing NO, the magnetization of the Rh atoms is quenched. Out of the six Rh atoms present in the unit cell, the spin polarization of each of the two Rh atoms to which N is attached is negligible, while the spin polarization of those atoms to which O is attached is reduced by about 81% and the spin polarization of the two Rh atoms which are furthest from the NO is reduced by about 28%. Similar effects have also been observed previously by us for NO adsorbed on small Rh clusters[33] and by Hass *et al.*[34] in their studies of NO adsorption on a hypothetical monolayer of Rh atoms. Apart from the fact that the latter group of authors worked with a monolayer of Rh (i.e., there was no substrate), there are other differences between our calculations and theirs: they did the calculations for NO adsorbing in the VB geometry alone, fixed the Rh-Rh distance at the value for bulk Rh, and did not relax the coordinates of NO. While they found that the magnetic moments on all the atoms of the monolayer are negligible, we find that the magnetism of those Rh atoms which are attached to the NO molecule is very strongly suppressed, while in the other Rh atoms there is a slight reduction.

As in the previous cases, the magnitude of E_{ads} increases upon performing an NSP calculation. One obtains values of −4.38 and −3.93 eV for the HH and VB configurations, respectively.

Upon coadsorbing NO on this Rh/MgO slab, we find that it is preferable for both the N and O to be at NN hollow sites

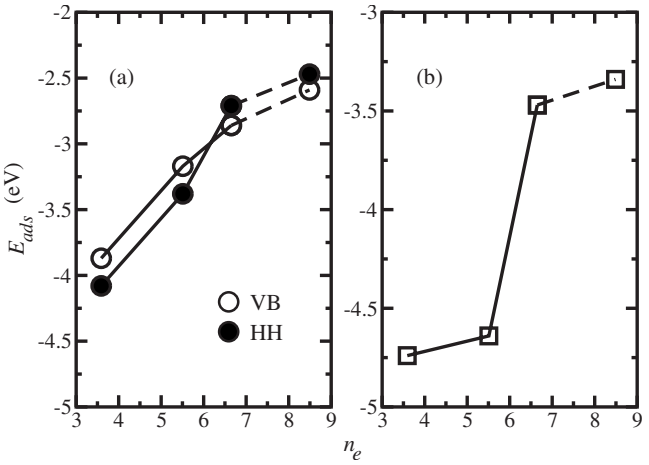

FIG. 6. Variation in (a) adsorption energy of NO, E_{ads}, and (b) coadsorption energy of N and O, with effective coordination n_e. The open and filled circles in (a) represent the vertical bridge and horizontal hollow adsorption geometries, respectively. The squares in (b) represent the coadsorption energy for the lowest-energy configuration of all geometries considered by us.

rather than at NN bridge sites. The former leads to a coadsorption energy of −4.74 eV, while the latter leads to a coadsorption energy of −4.10 eV.

IV. DISCUSSION OF TRENDS

We have seen that as we go from case (i) to case (iv), the effective coordination n_e decreases progressively and significantly. This decrease in effective coordination is accompanied by (and, in our interpretation, causes) a significant increase in the strength of adsorption of NO and coadsorption of N and O. Our main results are encapsulated in Fig. 6. In the panel on the left-hand side, we have presented our results for the adsorption energy of NO on these systems. The open circles represent results for the vertical bridge geometry, and the filled circles represent those for the horizontal hollow geometry. The following features are evident from this graph: (a) for a given geometry, the magnitude of E_{ads} increases monotonically as n_e is decreased; (b) the slope of this graph is larger for the HH than for the VB; this can be rationalized as being due to the fact that for the HH, both N and O are bonded to Rh atoms, whereas for the VB, only N is bonded to Rh atoms; (c) as a consequence of this the HH geometry becomes more favorable at lower n_e; and (d) the slope of the lines connecting cases (i) and (ii) is less than that connecting (ii), (iii), and (iv). This last observation can be attributed to the fact that in case (i) the substrate is nonmagnetic, whereas in case (ii) it is magnetic. In the absence of magnetism, adsorption is stronger and the points corresponding to cases (ii), (iii), and (iv) would be shifted downwards, and one would have obtained a roughly straight line connecting the points from the four cases considered by us. Since these three points have, however, been shifted upwards by the presence of magnetism, the slope connecting (i) and (ii) is reduced. The main conclusion from this graph is that the adsorption energy scales more or less linearly with effective coordination; we note further that the Rh(111) surface has a larger n_e (9.15) and weaker E_{ads} (−2.18 eV) than all four cases considered by us.

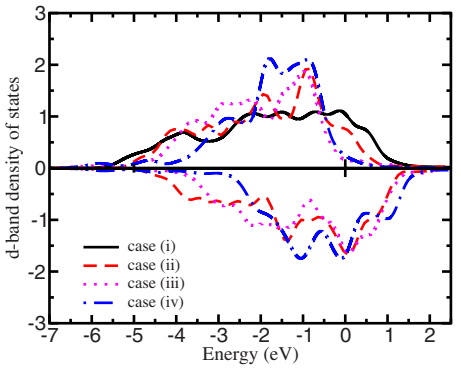

FIG. 7. (Color online) Rh d-band projected density of states (DOS) for the four cases. Positive and negative values denote the DOS for spin-up and spin-down electrons, respectively.

Similar conclusions about coadsorption can be drawn from the right-hand side panel, where the coadsorption energy is found to vary monotonically with n_e. The variation is less linear for this case, presumably because of changes in coadsorption geometry.

The adsorption energy decreases as we go from (i) to (iv) due to two reasons: (a) the strength of adsorption increases as the coordination is decreased, and (b) the horizontal hollow geometry, which leads to stronger binding to the substrate and a weaker and longer NO bond, becomes more favored at low effective coordination. However, these effects would have been even more marked if the substrate were to remain nonmagnetic: in every case, we have seen that NSP calculations (where magnetism is suppressed) point to stronger adsorption than SP calculations. For the VB geometry, the N–O bond length is found to be ~1.2 Å, whereas for the HH geometry, the bond length is increased to ~1.3 Å, suggesting that it should be easier to break the N–O bond in the latter case.

Our results show that strain and the presence of the oxide substrate contribute to the increased strength of adsorption primarily through their effect on n_e and that both effects contribute to roughly the same extent. In the case of the magnesia substrate considered by us, charge transfer plays a negligible role since the donation and back-donation mechanisms essentially cancel out. This may not be true for more active oxide substrates, such as titania and ceria.

It seems intuitively obvious that when Rh atoms have a lower effective coordination, they will bind adsorbates more strongly, thus making it easier to break bonds within the adsorbate. An alternative and equivalent way of looking at this effect is to consider the effect of lower coordination on the density of states. In Fig. 7, we show how the spin-polarized d-band density of states of the surface Rh atoms changes as we go from case (i) to case (iv)—it can be seen that the lowering of n_e results in a progressive narrowing of the d band. As mentioned earlier, the d-band width and position of the d-band center have been shown to be a good predictor of catalytic activity.[4]

In Fig. 8(a) we show how the position of the d-band center shifts with effective coordination. We see that as we go

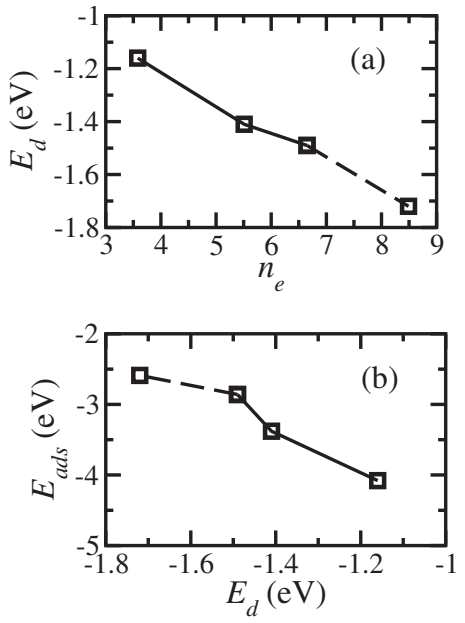

FIG. 8. Variation in (a) the position of the *d*-band center (E_d) with effective coordination and (b) the adsorption energy E_{ads} with E_d. In both cases, a monotonic and approximately linear relationship is observed. The points plotted correspond to the lowest-energy configuration for each case.

from case (i) to case (iv), the reduction in n_e is accompanied by an approximately linearly proportional shift in the *d*-band center, bringing it closer to the Fermi level. In Fig. 8(b) we show that the adsorption energy varies in a monotonic (and approximately linear) way with the *d*-band center.

V. SUMMARY AND CONCLUSIONS

We have studied the adsorption of NO and the coadsorption of N and O on strained and unstrained Rh surfaces with and without the presence of an MgO substrate. Both strain and placing a monolayer of Rh atoms on the oxide substrate lead to a significant lowering in the effective coordination of surface Rh atoms; doing both [i.e., placing a monolayer of Rh atoms pseudomorphically on an MgO(100) substrate] leads to the largest decrease in effective coordination n_e. Further, both the strain and the presence of the substrate (either separately or together) have the effect of making the surface Rh atoms magnetic. Every decrease in n_e is accompanied by (and, presumably, causes) a decrease in the *d*-band width of Rh atoms, a shift of the *d*-band center toward the Fermi level, and a strengthening of the adsorption of NO and the coadsorption of N and O. Thus for our systems the effective coordination appears to control surface reactivity. The extension of the present study to more systems would establish how general this relationship is.

We note that the effective coordination n_e is a quantity that can be very simply computed, especially if the structure is known—it is not even necessary to perform an *ab initio* density-functional theory calculation in order to compute it. Therefore it can serve as a simple guide or rule of thumb in order to design systems where the strength of adsorption or coadsorption takes on a desired value.

Thus, lowering the effective coordination seems to be a good strategy to increase the strength of adsorption and coadsorption and, thus, conceivably lower the barrier to dissociation of the NO bond. One can think of several ways of reducing effective coordination: e.g., by using rough surfaces, by placing Rh atoms on an inert oxide substrate, and by using Rh nanocatalysts where the Rh particles are sufficiently small so as to be significantly undercoordinated. However, most of these strategies to reduce n_e also favor magnetism, which competes with bonding.[33] This suggests that an optimal value of n_e should be aimed for, where the coordination is low enough so as to favor a significant strengthening of Rh–NO bonds and weakening of the N–O bond, yet the adverse effects of magnetism are not too evident. We are in the process of computing dissociation barriers in order to verify our expectation that lowering effective coordination will also weaken the N–O bond and thus catalyze the reduction of NO to N_2.

ACKNOWLEDGMENTS

We acknowledge funding from the Indo-Italian Programme of Cooperation in Science and Technology, administered by the Indian Dapartment of Science and Technology and the Italian MAE.

[1] D. Loffreda, D. Simon, and P. Sautet, J. Catal. **213**, 211 (2003).
[2] D. Loffreda, D. Simon, and P. Sautet, J. Chem. Phys. **108**, 6447 (1998).
[3] J. K. Norskov *et al.*, J. Catal. **209**, 275 (2002).
[4] B. Hammer and J. K. Norskov, Surf. Sci. **343**, 211 (1995).
[5] M. S. Daw and M. I. Baskes, Phys. Rev. Lett. **50**, 1285 (1983).
[6] M. S. Daw, Phys. Rev. B **39**, 7441 (1989).
[7] K. W. Jacobsen, J. K. Norskov, and M. J. Puska, Phys. Rev. B **35**, 7423 (1987).
[8] F. Ercolessi, E. Tosatti, and M. Parrinello, Phys. Rev. Lett. **57**, 719 (1986).
[9] A. Baraldi, L. Bianchettin, E. Vesselli, S. de Gironcoli, S. Lizzit, L. Petaccia, G. Zampieri, G. Comelli, and R. Rosei, New J. Phys. **9**, 143 (2007).
[10] I. Morrison, D. M. Bylander, and L. Kleinman, Phys. Rev. Lett. **71**, 1083 (1993).
[11] S. C. Wu, K. Garrison, A. M. Begley, F. Jona, and P. D. Johnson, Phys. Rev. B **49**, 14081 (1994).
[12] J. H. Cho and M. Scheffler, Phys. Rev. Lett. **78**, 1299 (1997).
[13] S. K. Nayak, S. E. Weber, P. Jena, K. Wildberger, R. Zeller, P. H. Dederichs, V. S. Stepanyuk, and W. Hergert, Phys. Rev. B **56**, 8849 (1997).
[14] J. H. Cho and M. H. Kang, Phys. Rev. B **52**, 13805 (1995).
[15] O. Eriksson, R. C. Albers, and A. M. Boring, Phys. Rev. Lett.

66, 1350 (1991).
[16] M. J. Zhu, D. M. Bylander, and L. Kleinman, Phys. Rev. B **43**, 4007 (1991).
[17] R. Wu and A. J. Freeman, Phys. Rev. B **45**, 7222 (1992).
[18] B. V. Reddy, S. N. Khanna, and B. I. Dunlap, Phys. Rev. Lett. **70**, 3323 (1993).
[19] D. Loffreda, F. Delbecq, D. Simon, and P. Sautet, J. Chem. Phys. **115**, 8101 (2001).
[20] S. Baroni, A. D. Corso, S. de Gironcoli, and P. Giannozzi, http://www.quantum-espresso.org/
[21] D. Vanderbilt, Phys. Rev. B **41**, 7892 (1990).
[22] J. P. Perdew, K. Burke, and M. Ernzerhof, Phys. Rev. Lett. **77**, 3865 (1996).
[23] M. Methfessel and A. T. Paxton, Phys. Rev. B **40**, 3616 (1989).
[24] H. J. Monkhorst and J. D. Pack, Phys. Rev. B **13**, 5188 (1976).
[25] N. W. Ashcroft and N. D. Mermin, *Introduction to Solid State Physics*, 5th ed. (Wiley & Sons, Texas, 1976).
[26] F. Bondino, G. Comelli, A. Baraldi, E. Vesselli, R. Rosei, A. Goldoni, S. lizzit, C. Bungaro, S. de Gironcoli, and S. Baroni, J. Chem. Phys. **119**, 12525 (2003).
[27] S. Nokbin, J. Limtrakul, and K. Hermansson, Surf. Sci. **566–568**, 977 (2004).
[28] R. W. G. Wyckoff, *Crystal Structures*, 2nd ed. (Interscience, New York, 1964).
[29] B. Johnson, P. M. W. Gill, and J. A. Pople, J. Chem. Phys. **98**, 5612 (1993).
[30] G. Teeter and J. L. Erskine, Surf. Rev. Lett. **6**, 813 (1999).
[31] A. Bogicevic and D. R. Jennison, Phys. Rev. Lett. **82**, 4050 (1999).
[32] C. Castleton, S. Nokbin, and K. Hermansson, Surf. Sci. **601**, 1218 (2007).
[33] P. Ghosh, R. Pushpa, S. de Gironcoli, and S. Narasimhan, J. Chem. Phys. **128**, 194708 (2008).
[34] K. C. Hass, M.-H. Tsai, and R. V. Kasowski, Phys. Rev. B **53**, 44 (1996).